Observational Study

Medicine

OPEN

TYROBP as a molecular target in cholangiocarcinoma, renal cancer and abdominal aortic aneurysm

Wei Jia, MD[a], Lei Chen, MD[b], Shiyang Hou, MD[a,*], Chunbo Kang, MD[a], Hongru Deng, MD[b]

Abstract

Cholangiocarcinoma occurs when there is a malignant tumor in the bile duct system. Renal cancer originates from renal tubular epithelial cells. Abdominal aortic aneurysm (AAA) is a permanently localized dilation caused by a lesion or injury to abdominal aortic wall. However, the relationship between TYROBP and cholangiocarcinoma, renal cancer and AAA remains unclear. The profiles of cholangiocarcinoma dataset GSE107943, renal cell carcinoma dataset GSE213324, and AAA dataset GSE47472 were downloaded from the GEO database using the platforms GPL18573, GPL24676, and GPL10558. DEGs were screened, WGCNA was performed as well as construction and analysis of PPI network. Functional enrichment analysis, GSEA, heat map of gene expression, survival analysis, and immune infiltration analysis were performed. The most relevant diseases to core genes were found by CTD. The GSE107943 dataset identified 3383 DEGs for cholangiocarcinoma, GSE47472 identified 95 DEGs for abdominal aortic aneurysm, and GSE213324 identified 10245 DEGs for renal cell carcinoma. For the GSE107943 cholangiocarcinoma dataset, GO analysis revealed enrichment in immune response, cell adhesion, extracellular space, and oxidoreductase activity. KEGG analysis indicated enrichment in metabolic pathways, the PI3K-Akt signaling pathway, cell apoptosis, the cell cycle, and the NF-kappa B signaling pathway. In the GSE47472 AAA dataset, GO analysis showed enrichment in neuroblast differentiation, cardiac muscle myofilament complex, and alkaline binding. KEGG analysis indicated enrichment in mRNA surveillance pathway and purine metabolism. In the GSE213324 renal cell carcinoma dataset, GO analysis indicated enrichment in immune system processes, cell adhesion, and membrane parts. KEGG analysis showed enrichment in cytokine-cytokine receptor interaction, calcium signaling pathway, and hematopoietic cell lineage. Furthermore, for cholangiocarcinoma (GSE107943), enriched terms associated with DEGs were in metabolic pathways, cell apoptosis, and the cell cycle. For AAA (GSE47472), enriched terms were in alkaline binding and cellular redox homeostasis. For renal cell carcinoma (GSE213324), enriched terms were in biological adhesion, regulation of immune system processes, and cell surface. Common core genes (ADH6, AGXT, CYP3A43, TYROBP) were identified for cholangiocarcinoma, renal cell carcinoma, and AAA. ADH6 and TYROBP were associated with cholangiocarcinoma, AAA, renal tumors, kidney diseases, atherosclerosis, and inflammation. TYROBP is abnormally expressed in cholangiocarcinoma, renal cancer and abdominal aortic aneurysm.

Abbreviations: AAA = abdominal aortic aneurysm, CTD = comparative toxicogenomics database, DEGs = differentially expressed genes, GEO = gene expression omnibus, GO = gene ontology, GSEA = gene set enrichment analysis, KEGG = Kyoto Encyclopedia of genes and genomes, PPI = protein-protein interaction, STRING = Search Tool for the Retrieval of Interacting Genes, WGCNA = weighted gene co-expression network analysis.

Keywords: abdominal aortic aneurysm, bioinformatics, cholangiocarcinoma, prognosis, renal cancer, TYROBP

1. Introduction

Cholangiocarcinoma refers to a common malignant tumor originating from the bile duct, including the extrahepatic bile duct from the hepatic hilum to the distal common bile duct.[1] It is more prevalent in middle-aged and elderly individuals, with insidious onset, lack of specific clinical manifestations, and often invasion of the bile duct by the tumor.[2] Early metastasis is relatively uncommon, mainly involving infiltration and direct spread along the bile duct wall in an upward and downward direction. Clinical management options include surgical treatment, radiotherapy, and chemotherapy. Novel therapeutic

The authors have no funding and conflicts of interest to disclose.

The datasets generated during and/or analyzed during the current study are available from the corresponding author on reasonable request.

The data in this article are from public databases and are exempt from ethical review.

[a] Gastrointestinal Rehabilitation Center, Beijing Rehabilitation Hospital, Capital Medical University, Beijing, P. R. China, [b] Department of Vascular Surgery, Fuxing Hospital Affiliated to Capital Medical University, Beijing, P. R. China.

**Correspondence: Shiyang Hou, Gastrointestinal rehabilitation center, Beijing Rehabilitation Hospital, Capital Medical University, Badachu Xixia Village, Shijingshan District, Beijing, 100144, P.R. China (e-mail: houshiyang23117@163.com).*

How to cite this article: Jia W, Chen L, Hou S, Kang C, Deng H. TYROBP as a molecular target in cholangiocarcinoma, renal cancer and abdominal aortic aneurysm. Medicine 2024;103:1(e36843).

Received: 5 September 2023 / Received in final form: 8 December 2023 / Accepted: 12 December 2023

http://dx.doi.org/10.1097/MD.0000000000036843

approaches include photodynamic therapy and intracavitary radiofrequency ablation.[3] However, the prognosis is generally poor. In early cases, surgical resection is the primary treatment, often followed by adjuvant radiotherapy and chemotherapy to consolidate and enhance the surgical outcomes. For advanced cases where surgical resection is not feasible, biliary drainage procedures should be performed to control biliary infections, improve liver function, reduce complications, prolong life, and enhance the quality of life.[4,5] Renal cancer is a malignant tumor originating from renal cells. Renal cancer usually develops in people over the age 50, with a higher incidence in men than in women, and the risk is about twice as high in smokers, genetic factors, chronic kidney disease, obesity may increase the risk of kidney cancer.[6,7] Renal cancer has a predilection for the elderly, and has a certain familial hereditary predisposition to kidney cancer. Early stage renal cancer is usually asymptomatic and difficult to detect. When tumors increase in size or metastasize, symptoms such as hematuria, low back or abdominal pain, masses, weight loss, fever, fatigue, fractures, or bone pain may develop.[8] The pathologic types of RCC include RCC, transitional cell carcinoma, sarcoma, and childhood Wilms tumor, among others, and will usually be classified as grades I-IV. In RCC, the tumor cells have morphologies typical of clear cells, granulosa cells, and papillary cells.[9,10] Renal cancer is a relatively harmful malignancy with high invasiveness and metastasis, and patients often experience pain and discomfort. Abdominal aortic aneurysm refers to a locally dilated, formed vasculopathy of the abdominal aorta that occurs in its mural layer. The abdominal aortic aneurysm is a common vascular disease that usually occurs in elderly over 60 years of age, is about 3 times more prevalent in men than in women, twice the risk in smokers, and has a higher incidence in developed countries such as Europe and the United States.[11–13] Early asymptomatic, slow growth rate, high insidious, easy rupture of abdominal aortic aneurysm will lead to severe internal bleeding, with a high mortality rate of more than 80%.[14] Early abdominal aortic aneurysms are usually asymptomatic, and as abdominal aortic aneurysms grow, abdominal discomfort, low back pain, pulse abnormalities, palpitations, shortness of breath, change in appearance, sudden pain, and other symptoms occur. The pathological features of abdominal aortic aneurysm (AAA) are associated with abnormal dilatation of arterial wall, stratification of layers of the vessel wall, fibrosis of the vessel wall, thrombosis, and rupture of the aneurysm.[15] Abdominal aortic aneurysm has a great harm, abdominal aortic aneurysm rupture causes massive internal bleeding, thrombosis blocks blood vessels, with the enlargement of abdominal aortic aneurysm compressing surrounding tissues.

Bioinformatics is an interdisciplinary field that involves computer science, mathematics, biology, and statistics. The development of bioinformatics technology has greatly assisted biological research, accelerating the interpretation and understanding of biomolecules such as genomes, proteins, and metabolomes. Bioinformatics technology includes sequence analysis, structure analysis, functional prediction, systems biology, genomics, and proteomics. Bioinformatics technology is constantly evolving, allowing for more efficient and accurate interpretation of biological information. The advantages of bioinformatics technology are mainly reflected in its efficiency, accuracy, visualization, and reproducibility.

However, at present the relationship between the TYROBP gene and cholangiocarcinoma, renal cancer and abdominal aortic aneurysm is unknown. Therefore, the study intends to use the bioinformatics technology to mine the core genes, and correlation analysis was performed. The public datasets were used to validate significant role of TYROBP gene in cholangiocarcinoma, renal cancer and abdominal aortic aneurysm. And the basal cell experiment was applied to verify it.

2. Method

2.1. Cholangiocarcinoma, renal cancer and abdominal aortic aneurysm datasets

In this study, the profiles of cholangiocarcinoma dataset GSE107943, renal cell carcinoma dataset GSE213324, and abdominal aortic aneurysm dataset GSE47472 were downloaded from the GEO database (http://www.ncbi.nlm.nih.gov/geo/) using the platforms GPL18573, GPL24676, and GPL10558, respectively. GSE107943 consists of 30 cholangiocarcinoma samples and 27 normal samples. GSE213324 includes 21 renal cell carcinoma samples and 20 normal samples. GSE47472 comprises 14 abdominal aortic aneurysm samples and 8 normal samples.

2.2. Differentially expressed genes (DEGs) were screened

Probe aggregation and background correction of merge matrix using R package "limma." *P* value were adjusted using Benjamini-Hochberg method. The multiple change (FC) is calculated using error detection rate (FDR). The cutoff value of DEG is *P* less than .05 and FC is greater than 1.5. And make a visual representation of the volcano.

2.3. Weighted gene co-expression network analysis (WGCNA)

First of all, use de-batch and post-merge matrix to calculate Median Absolute Deviation of each gene. The good sample gene method of WGCNA in R package was used to remove outlier genes and samples to construct a scale-free co-expression network. To classify genes with similar expression profiles into gene modules, we performed average linkage hierarchical clustering on the gene dendrogram based on the Topological Overlap Measure (TOM) with a minimum gene group size of 30. A sensitivity threshold of 3 was set. For further module analysis, we computed differences between module characteristic genes, selected a cut line for the module dendrogram, and merged certain modules. Additionally, we merged modules with a distance less than 0.25. It is noteworthy that the gray module is considered a gene set that cannot be assigned to any module.

2.4. Protein-protein interaction (PPI) network

Search Tool for the Retrieval of Interacting Genes (STRING) is a search system for known and predicted PPI. The STRING also contains the predicted results using bioinformatics methods. The DEGs were input into the PPI network constructed by STRING and the core genes were predicted. The PPI network was visualized, core genes are predicted by Cytoscape software. First of all, we import PPI network into the Cytoscape, and then find the module with the best correlation through MCODE, and MCC and MNC were used to calculate the best correlated genes. Finally, the list of core genes was obtained after visualization.

2.5. Functional enrichment analysis

Gene Ontology (GO) analysis is a computational method to evaluate gene functions and biological pathways, and it is a key step to endow sequence information with practical biological significance. Kyoto Encyclopedia of Gene and Genome (KEGG) is an online database dedicated to collecting information on genomes, molecular interaction networks, enzyme catalytic pathways, and biochemical products. The genomic information and gene function were linked, and gene function was systematically analyzed. The list of differential genes screened

by Wayne map was input into KEGG rest API obtained latest KEGG Pathway gene annotation. Gene set enrichment results were obtained using R package cluster Profiler.

Metascape (http://metascape.org/) can realize cognition of gene or protein function, and can be visually exported. We used Metascape database to analyze functional enrichment of the above differential gene list and derive it.

2.6. Gene set enrichment analysis (GSEA)

GSEA is based on level-specific gene probes that evaluate data from microarrays and is a way to uncover genomic expression data through fundamental knowledge. Based on cholangiocarcinoma and normal samples, renal cell carcinoma and normal samples, abdominal aortic aneurysm and normal samples, the 3 sets of samples are divided into 2 groups each. Five is minimum gene set and 5000 is maximum gene set, 1000 resampling times. The whole genome was analyzed by GO and KEGG.

2.7. Gene expression heat map

We use the R-packet heatmap to map expression of core genes found in PPI network. Differential expression of core genes in cholangiocarcinoma, renal cell carcinoma, abdominal aortic aneurysm and normal samples were visualized.

2.8. Survival analysis

We obtained clinical survival data for renal cell carcinoma from TCGA and calculated the optimal cutoff value for the RiskScore of core genes using the R package maxstat (version: 0.7–25). The cutoff value was set with a minimum group sample size greater than 25% and a maximum sample size less than 75%. Based on this, we divided the samples into high and low groups. Further analysis was performed using the R package survival's survfit function to assess the prognostic differences between the 2 groups. The log-rank test method was employed to evaluate the significance of prognostic differences between samples in different groups. We observed whether each independent core gene had a significant impact on the prognosis of renal cell carcinoma.

Additionally, we conducted ROC analysis using the R package pROC (version 1.17.0.1). Patient follow-up times were utilized to perform ROC analysis at time points of 365, 1095, and 1825 days with the roc function of pROC. The ci function of pROC was employed to assess the AUC and confidence intervals to obtain the final AUC results, indicating the diagnostic value of the core gene prognostic score. Furthermore, we generated overall survival plots and box plots for cholangiocarcinoma to visualize the impact of core genes in cholangiocarcinoma.

2.9. Immune infiltration analysis

The CIBERSORT is a very common method for calculating immune cell infiltration. We applied the integrated bioinformatics method, used the CIBERSORT software package to analyze the de-batch merging matrix, and immune cell abundance was estimated by deconvoluting the expression matrix of immune cell subtypes by linear support vector regression principle. At the same time, the samples with sufficient confidence were selected by using confidence $P < .05$ as the truncation criterion.

2.10. Comparative toxicogenomics database (CTD) analysis

CTD is a powerful public database, which predict gene/protein relationships with disease. We input core gene into CTD, find disease most related to the core gene. Excel was used to draw the radar map of differential expression of each gene.

3. Results

3.1. Analysis of DEGs

In this study, using the predefined cutoff values, DEGs were identified based on the matrices for cholangiocarcinoma, renal cell carcinoma, and abdominal aortic aneurysm. In the cholangiocarcinoma dataset GSE107943, 3383 DEGs were identified (Fig. 1A). For the abdominal aortic aneurysm dataset GSE47472, 95 DEGs were identified (Fig. 1B). In the renal cell carcinoma dataset GSE213324, 10245 DEGs were identified (Fig. 1C).

3.2. The functional enrichment analysis

3.2.1. DEGs. GO and KEGG analyses were conducted. For the DEGs identified in the cholangiocarcinoma dataset GSE107943. According to the GO analysis results, they are mainly enriched in immune response, cell adhesion, extracellular space, and oxidoreductase activity (Fig. 2A–C). As for the KEGG analysis results, the targeted cells are mainly enriched in metabolic pathways, the PI3K-Akt signaling pathway, cell apoptosis, the cell cycle, and the NF-kappa B signaling pathway (Fig. 2D).

For GSE47472, according to GO analysis, DEGs were mainly enriched in neuroblastic differentiation, cardiac troponin complex, and base binding (Fig. 3A–C). KEGG analysis showed that target cells were mainly enriched in mRNA monitoring pathway and purine metabolism (Fig. 3D).

For GSE213324, according to GO analysis, DEGs were mainly enriched in immune system processes, cell adhesion, and plasma membrane parts (Fig. 4A–C). KEGG analysis showed that the target cells were mainly enriched in interaction between cytokines and cytokine receptors, calcium signaling pathway, and hematopoietic cell lines (Fig. 4D).

3.2.2. GSEA. GSEA was performed to search for possible enrichment items among non-differentially expressed genes, and results of DEGs were verified. For the cholangiocarcinoma dataset GSE107943, the intersection of enriched terms between GO and KEGG pathways for the identified DEGs is shown in the figure. The main enrichment is observed in metabolic pathways, cell apoptosis, and the cell cycle (Fig. 2E–H).

For GSE47472, the intersection of enrichment terms and GO KEGG enrichment terms of DEGs was mainly enriched in base binding and cellular REDOX homeostasis (Fig. 3E–H).

For GSE213324, the intersection of enrichment terms and GO KEGG enrichment terms of DEGs was mainly enriched in biological adhesion, regulation of immune system processes, and cell surface (Fig. 4E–H).

3.3. Metascape enrichment analysis

In Metascape's enrichment analysis, differential genes from cholangiocarcinoma, renal cell carcinoma, and abdominal aortic aneurysm were subjected to GO enrichment analysis. The results indicate regulation of tumor necrosis factor production, PID FOXM1 pathway, and negative regulation of the immune system process (Fig. 5A). Additionally, we generated enrichment networks colored by enriched terms and *P* values (Fig. 5B and C), providing a visual representation of the associations and confidence levels of various enriched terms.

3.4. WGCNA

The network topology is analyzed and the soft threshold power of WGCNA is set to 6 (Fig. 6A and B). Hierarchical clustering trees were constructed for all genes, significant modules were

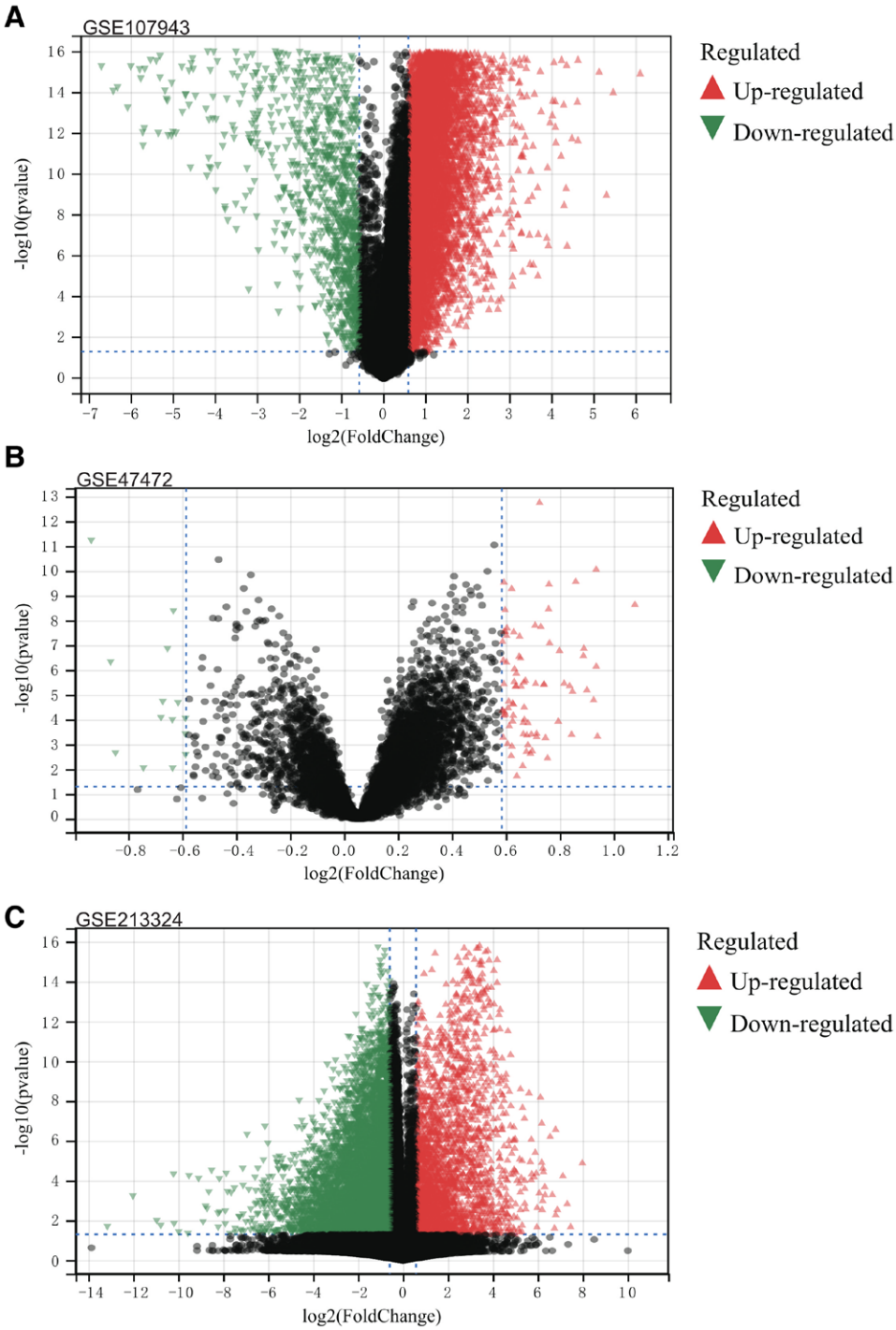

Figure 1. Analysis of differentially expressed genes. (A) Cholangiocarcinoma, 3383 DEGs were identified in GSE10794. (B) Abdominal aortic aneurysm, 95 DEGs were identified in GSE47472. (C) Renal cell carcinoma, 10245 DEGs were identified in GSE213324. DEGs = differentially expressed genes.

generated (Fig. 6C). The interaction between modules was analyzed (Fig. 6D). Heatmaps of the correlation between modules and phenotypes (Fig. 7A). Scatter plots of correlation between GS and MM were generated (Fig. 7B).

The calculation of the module eigengene (ME) and its correlation with gene expression was performed to obtain module membership (MM). Based on a cutoff criterion ($|MM| > 0.8$), 4916 highly connected genes were identified as hub genes within clinically significant modules. Additionally, a Venn diagram was generated using the intersection of genes selected by Weighted Gene Co-expression Network Analysis (WGCNA) and differentially expressed genes (DEGs). This intersection was utilized for the creation and analysis of protein-protein interaction networks (Fig. 7C).

3.5. Immune infiltration analysis

The analysis of the matrix was conducted using the CIBERSORT software package. At a 95% confidence level, the proportions of immune cells in the entire gene expression matrix were obtained (Fig. 8A), and a heatmap of the expression levels of immune cells in the dataset was generated (Fig. 8B). Furthermore, co-expression correlation analysis

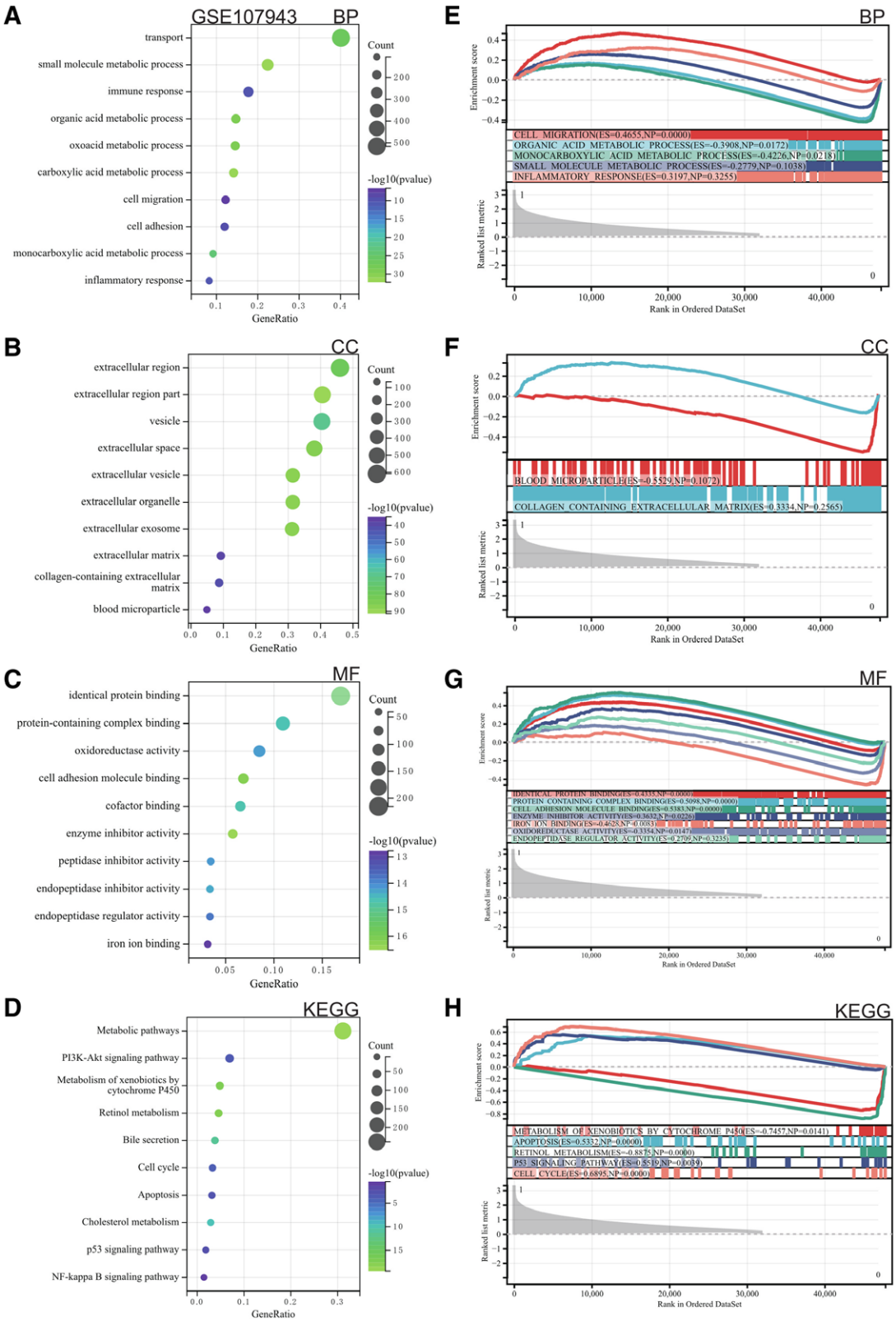

Figure 2. Functional enrichment analysis of cholangiocarcinoma. (A–C) GO. (D) KEGG. (E–H) GSEA. GO = gene ontology, GSEA = gene set enrichment analysis, KEGG = Kyoto Encyclopedia of genes and genomes.

was performed on infiltrating immune cells, resulting in a co-expression pattern diagram among immune cell components (Fig. 8C).

3.6. The PPI Network

We created Protein-Protein Interaction (PPI) networks for the differential genes of the 3 diseases. The PPI network for

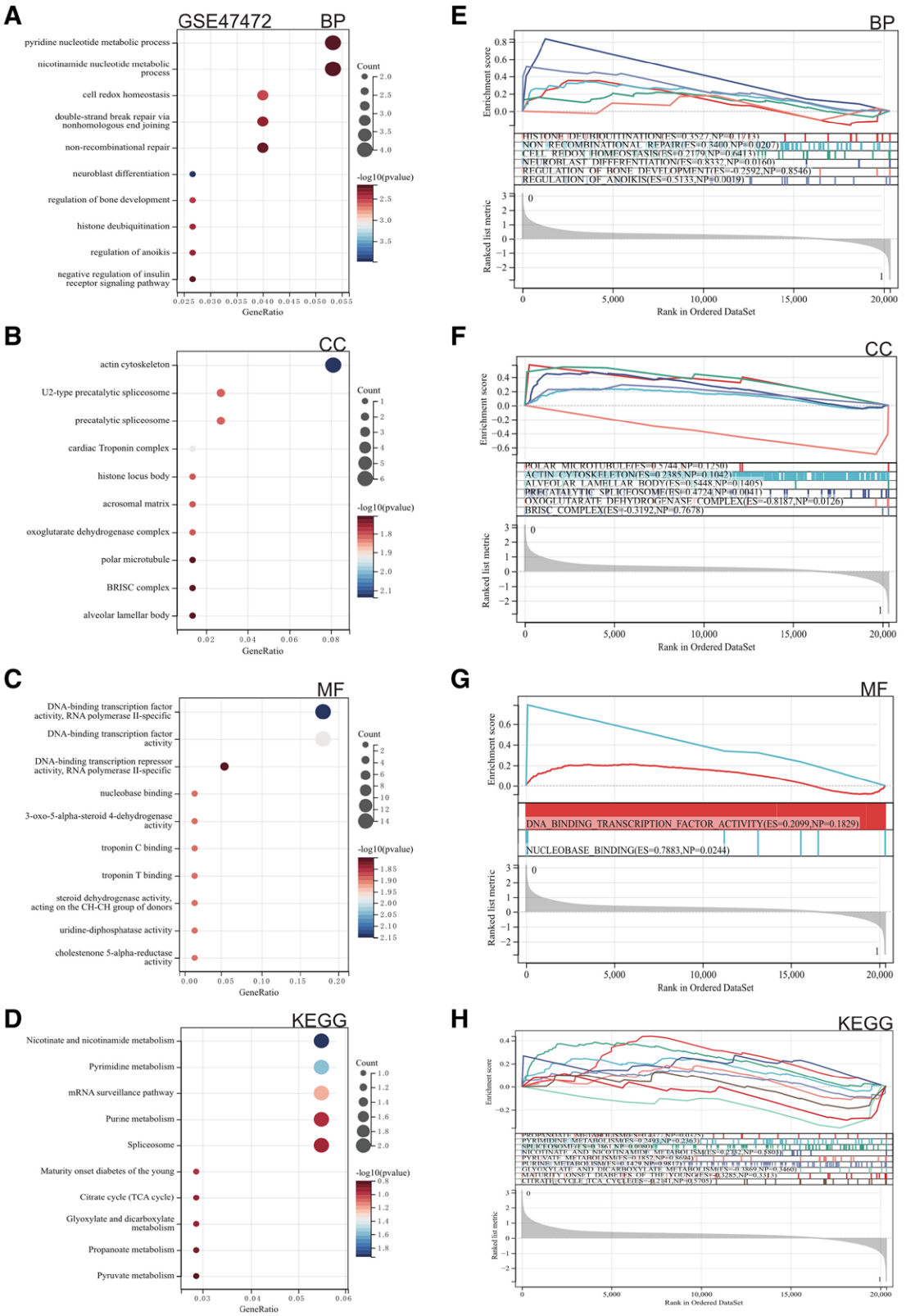

Figure 3. Functional enrichment analysis of abdominal aortic aneurysm. (A–C) GO. (D) KEGG. (E–H) GSEA. GO = gene ontology, GSEA = gene set enrichment analysis, KEGG = Kyoto Encyclopedia of genes and genomes.

GSE107943 is shown in Figure 9A, and the core gene cluster for cholangiocarcinoma was identified (Fig. 9B). Subsequently, the PPI network for GSE47472 was obtained (Fig. 9C), and core genes for abdominal aortic aneurysm were identified using the MCC algorithm (Fig. 9D). Next, the PPI network for GSE213324 was generated (Fig. 9E), and core genes for renal cell carcinoma were identified using the MCC algorithm (Fig. 9F). Finally, the intersection of core genes for the 3

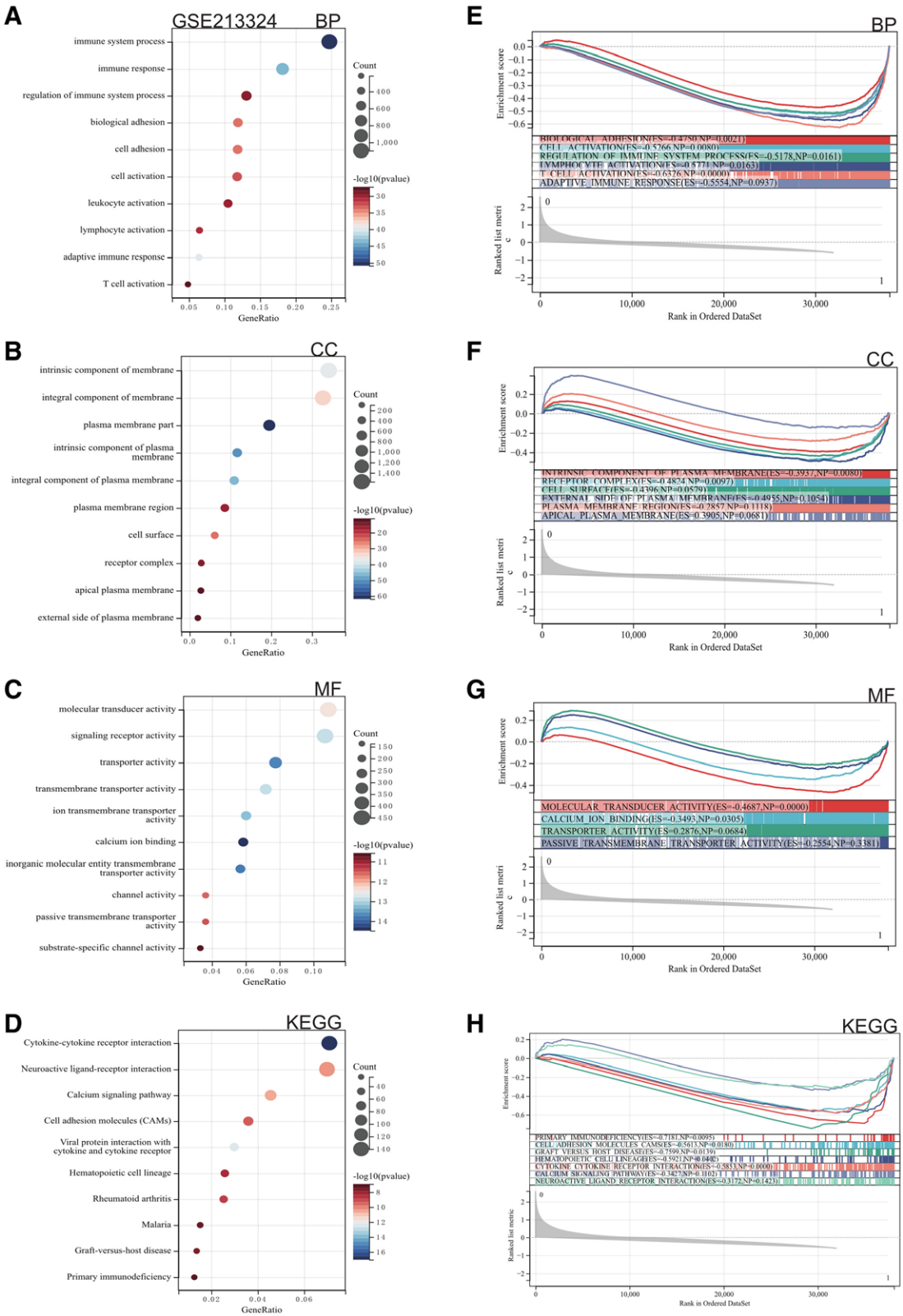

Figure 4. Functional enrichment analysis of renal cancer. (A–C) GO. (D) KEGG. (E–H) GSEA. GO = gene ontology, GSEA = gene set enrichment analysis, KEGG = Kyoto Encyclopedia of genes and genomes.

diseases was visualized in a Venn diagram (Fig. 9G), revealing common core genes (ADH6, AGXT, CYP3A43, TYROBP) in cholangiocarcinoma, renal cell carcinoma, and abdominal aortic aneurysm.

3.7. Survival analysis

Using survival data downloaded from TCGA, we generated survival-related results for cholangiocarcinoma and renal cell carcinoma. Firstly, we obtained the overall survival plot

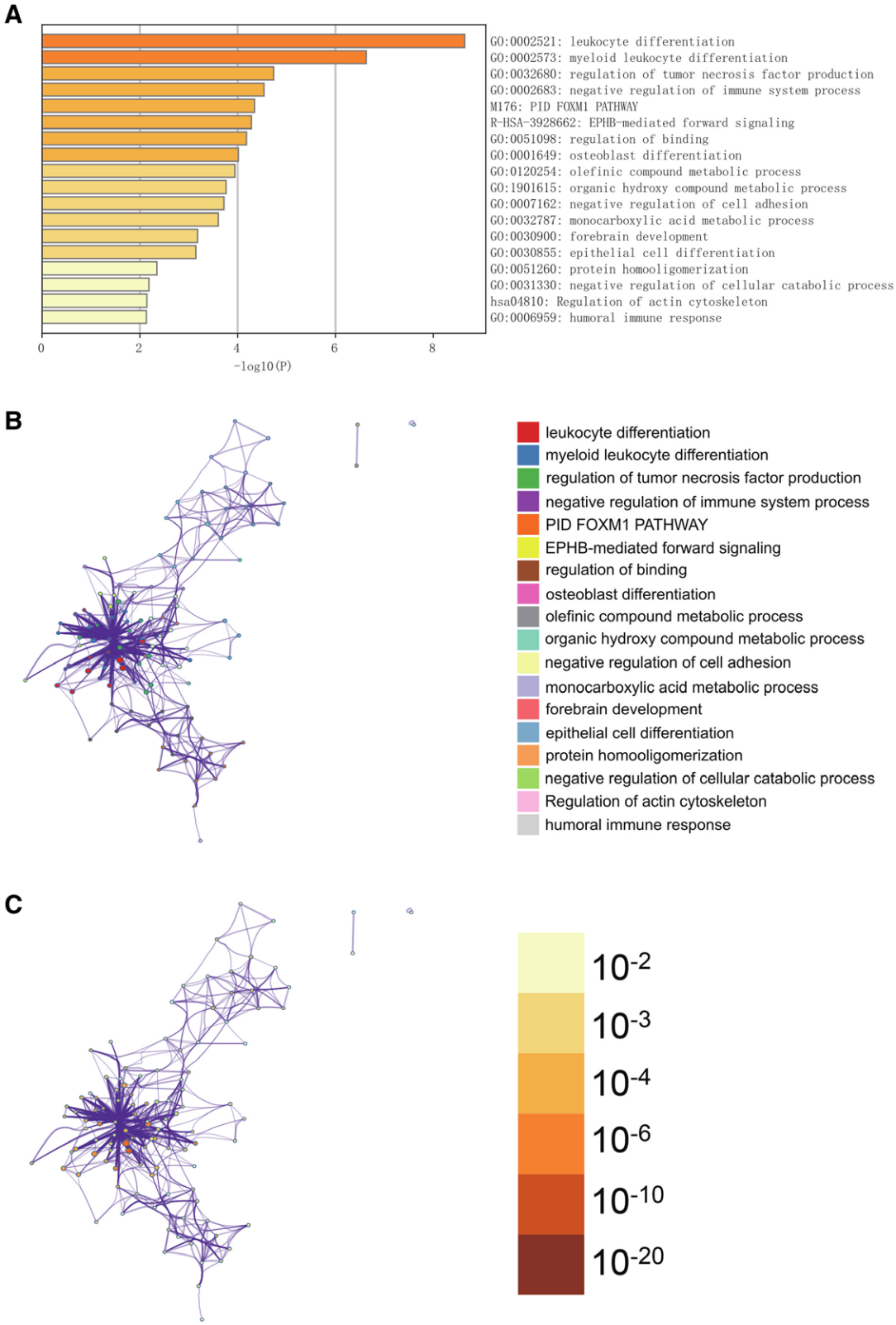

Figure 5. Metascape enrichment analysis. (A) In Metascape's enrichment analysis, differential genes from cholangiocarcinoma, renal cell carcinoma, and abdominal aortic aneurysm were subjected to GO enrichment analysis. The results indicate regulation of tumor necrosis factor production, PID FOXM1 pathway, and negative regulation of the immune system process (B) The enrichment network colored by enrichment terms (C) The enrichment network colored by *P* value (D) A visual representation of the associations and confidence levels of various enriched terms. GO = gene ontology.

(Fig. 10A) and box plot (Fig. 10B) for the core genes in cholangiocarcinoma. The results indicate differential expression of core genes between cholangiocarcinoma and normal samples, and their impact on the survival outcomes in cholangiocarcinoma. Next, we created a forest plot (Fig. 11A) and KM survival curve (Fig. 11B) for renal cell carcinoma, along with a box

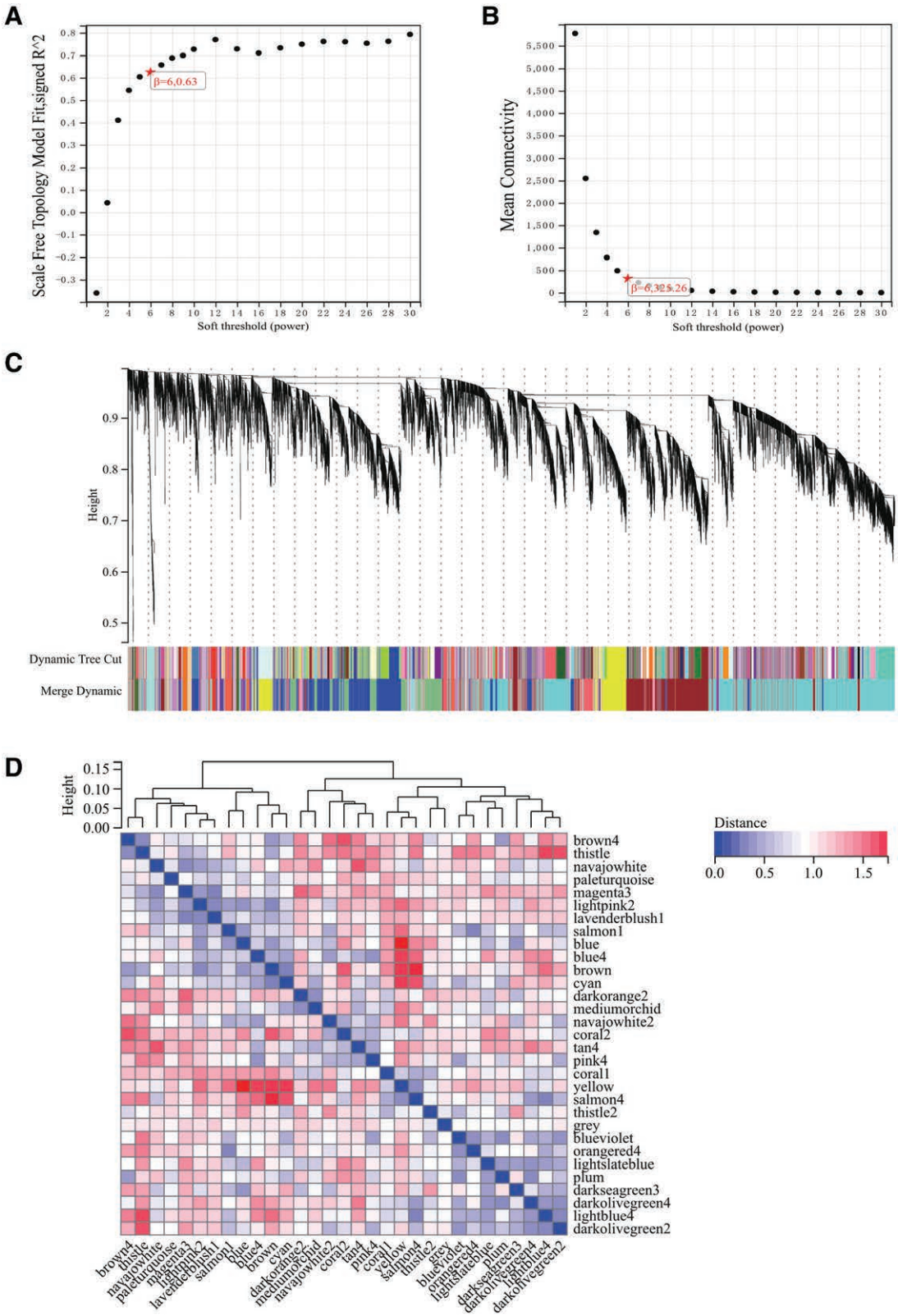

Figure 6. WGCNA. (A) β = 6, 0.63 (B) β = 6, 325.26 (C) Hierarchical clustering trees were constructed for all genes, significant modules were generated. (D) Interactions between these modules.

plot for the core genes (Fig. 11C). The results reveal significant differences in the expression of core genes between renal cell carcinoma and normal samples. Subsequently, we plotted the prognosis score relationship for renal cell carcinoma, observing a clear decrease in patient survival rates with increasing risk scores, where the low-risk group exhibited significantly higher survival time and rates than the high-risk group (Fig. 12A).

Visualizing the expression heatmap of core genes in renal cell carcinoma survival data, we found that the core gene (ADH6) acts as a protective factor, showing a downregulation

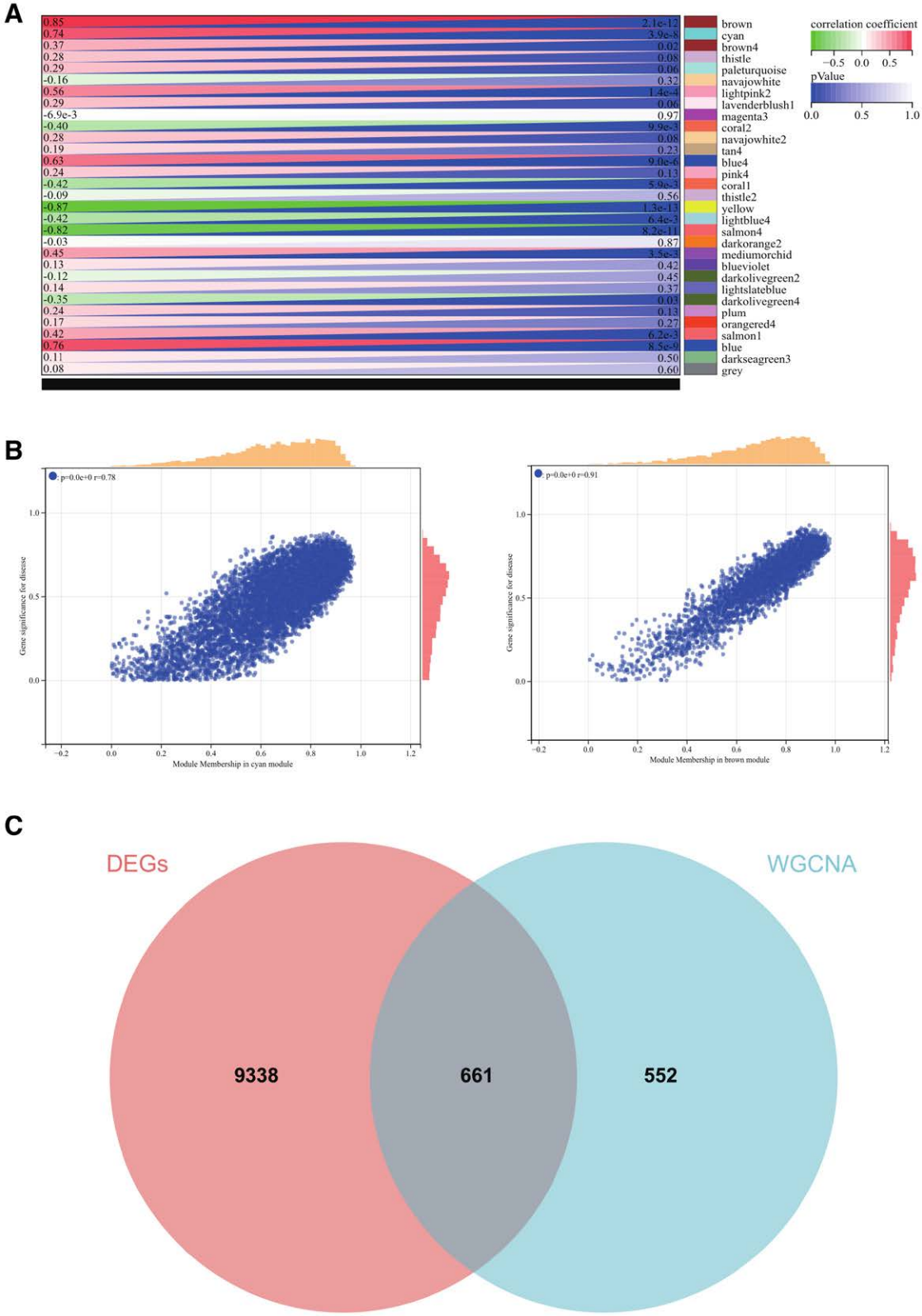

Figure 7. WGCNA. (A) Heatmaps of the correlation between modules and phenotypes. (B) Scatter plots of correlation between GS and MM. (Fig. 7C) Venn diagram was generated using the intersection of genes selected by WGCNA and DEGs. DEGs = differentially expressed genes, WGCNA = weighted gene co-expression network analysis.

trend with increasing risk scores. On the other hand, core genes (CYP3A43, TYROBP) act as risk factors, exhibiting an upregulation trend with increasing risk scores (Fig. 12B). Additionally, we generated ROC curves for the risk score, and the AUC values indicate that the risk score has predictive value (Fig. 12C).

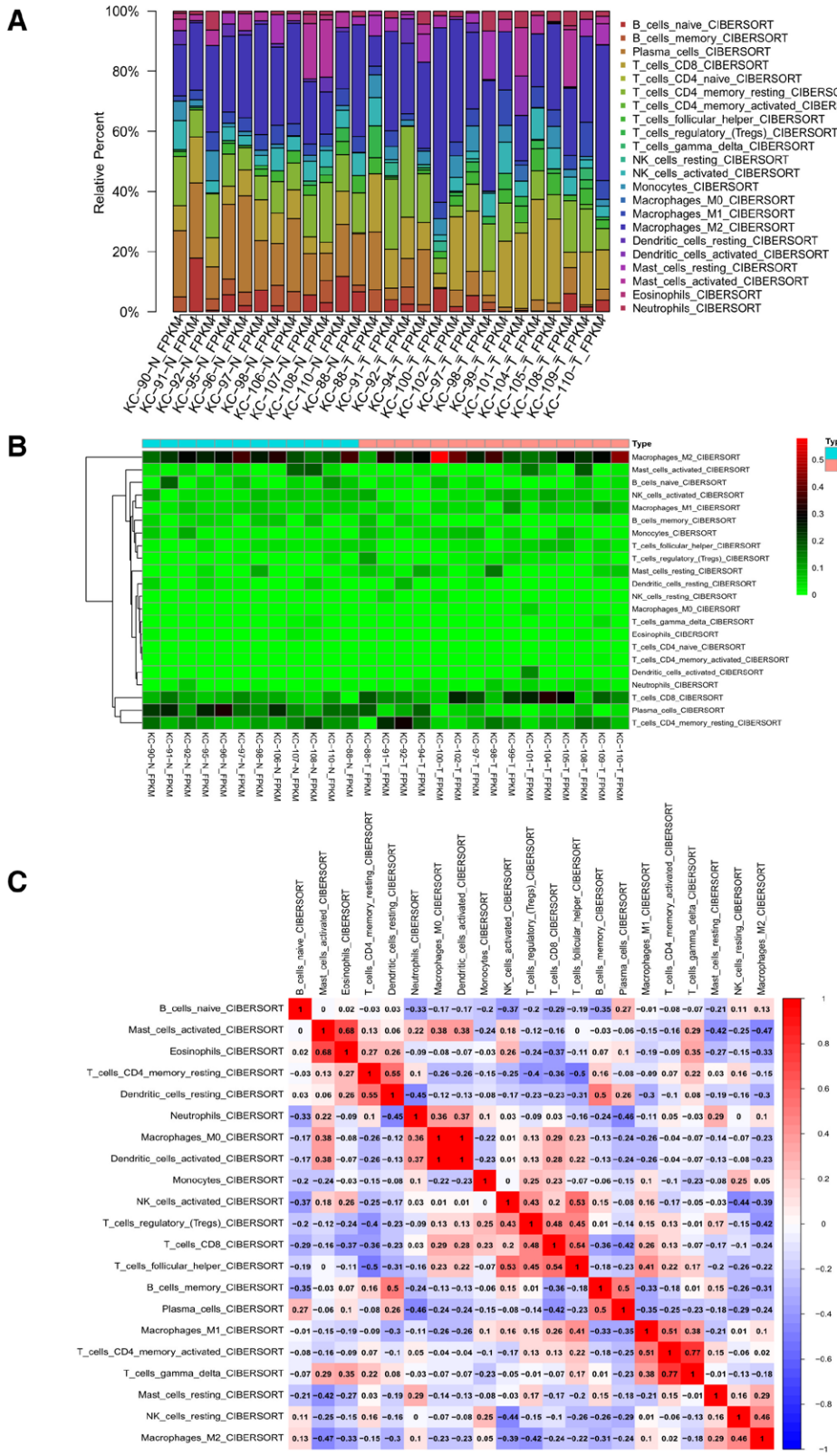

Figure 8. Immune infiltration analysis. (A) The proportions of immune cells in the entire gene expression matrix. (B) A heatmap of the expression levels of immune cells in the dataset. (C) co-expression pattern diagram among immune cell components.

3.8. Gene expression heat map

We visualized the expression heatmaps of core genes in the samples and observed significant differences in the expression levels of core genes (ADH6, TYROBP) between cholangiocarcinoma, renal cell carcinoma, and abdominal aortic aneurysm samples compared to normal samples (Fig. 13A–C). This suggests that the core genes (ADH6, TYROBP) may play a regulatory role in cholangiocarcinoma, renal cell carcinoma, and abdominal aortic aneurysm.

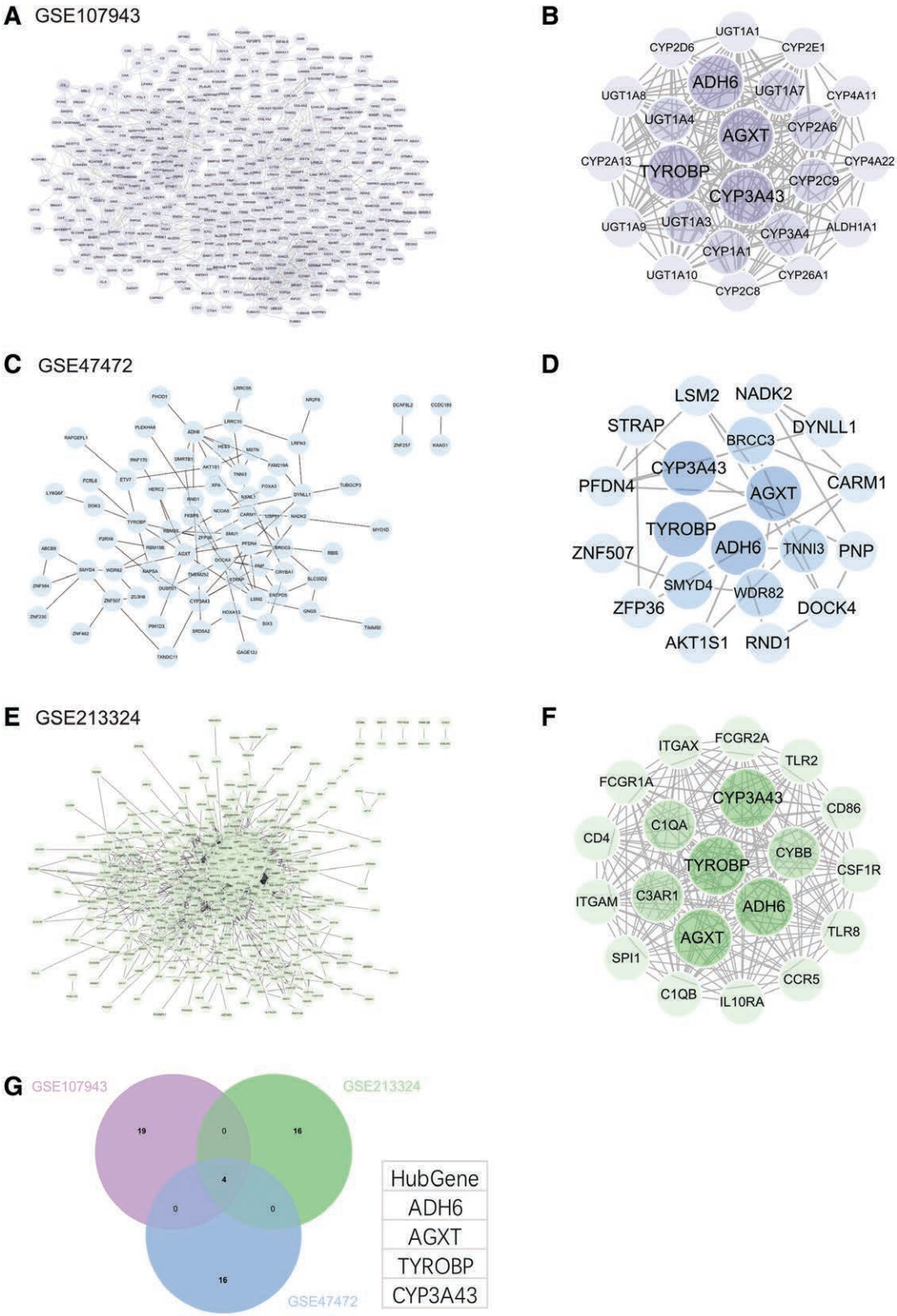

Figure 9. The PPI Network. (A) GSE107943. (B) The core gene cluster for cholangiocarcinoma. (C) GSE47472. (D)The core genes for abdominal aortic aneurysm were identified using the MCC algorithm. (E) GSE213324. (F) The core genes for renal cell carcinoma were identified using the MCC algorithm. (G)The intersection of core genes for the 3 diseases was visualized in a Venn diagram. PPI = protein-protein interaction.

3.9. The CTD analysis

In this study, we input the list of core genes into the CTD website to search for diseases related to these core genes, enhancing our understanding of the associations between genes and diseases. We discovered that the core genes (ADH6, TYROBP) are associated with cholangiocarcinoma, abdominal aortic aneurysm, renal tumors, kidney diseases, atherosclerosis, and inflammation (Fig. 13D). Combining the results of the above

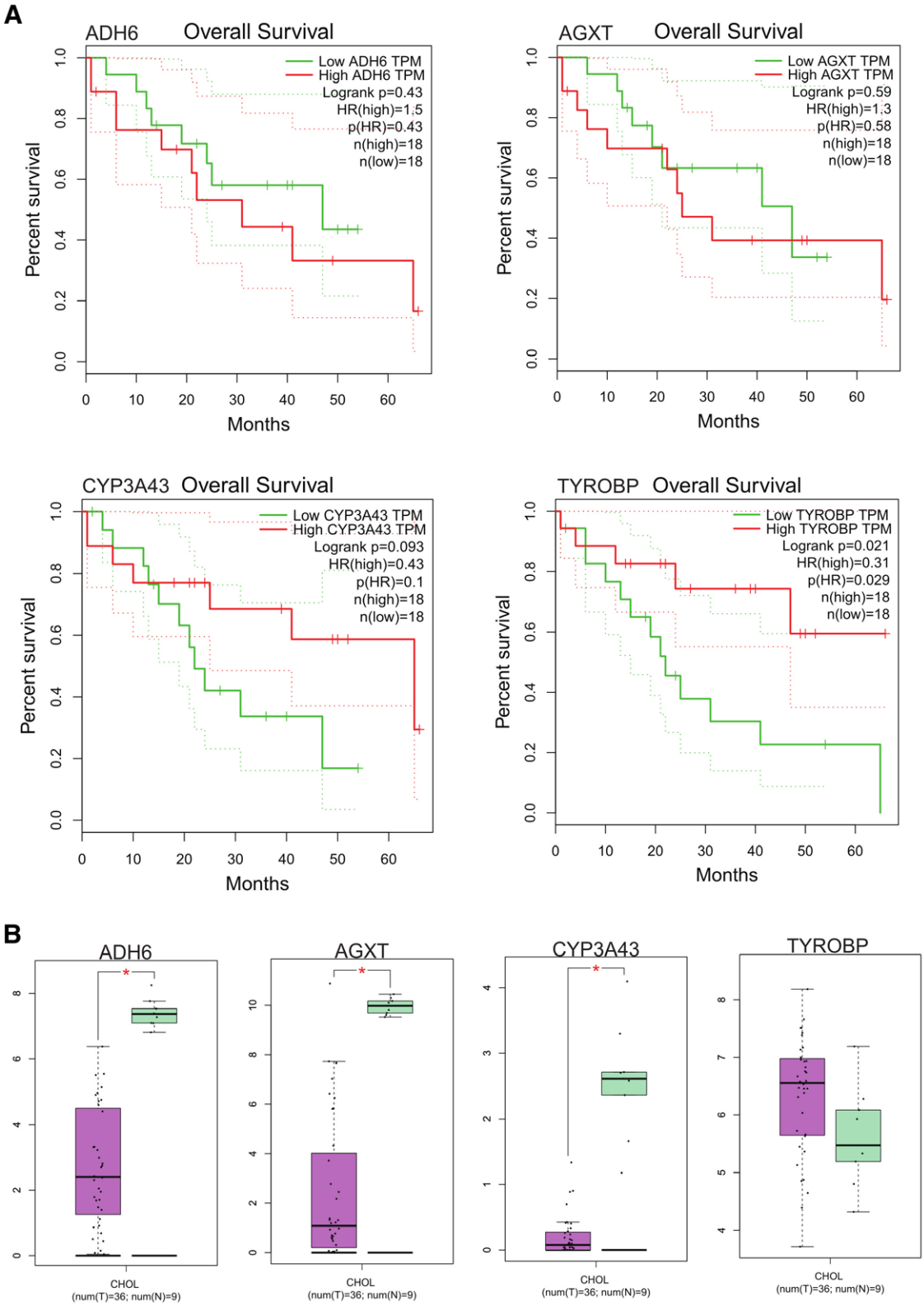

Figure 10. Survival analysis. (A) The overall survival plot. (B)The box plot.

analyses, we selected the core gene (TYROBP) that is significantly correlated with cholangiocarcinoma, renal cell carcinoma, and abdominal aortic aneurysm as the target gene for our study.

4. Discussion

Cholangiocarcinoma is a malignant tumor that grows in the bile ducts of the liver, exhibiting distinct regional prevalence with a slightly higher incidence in males.[16] Renal cancer is a relatively

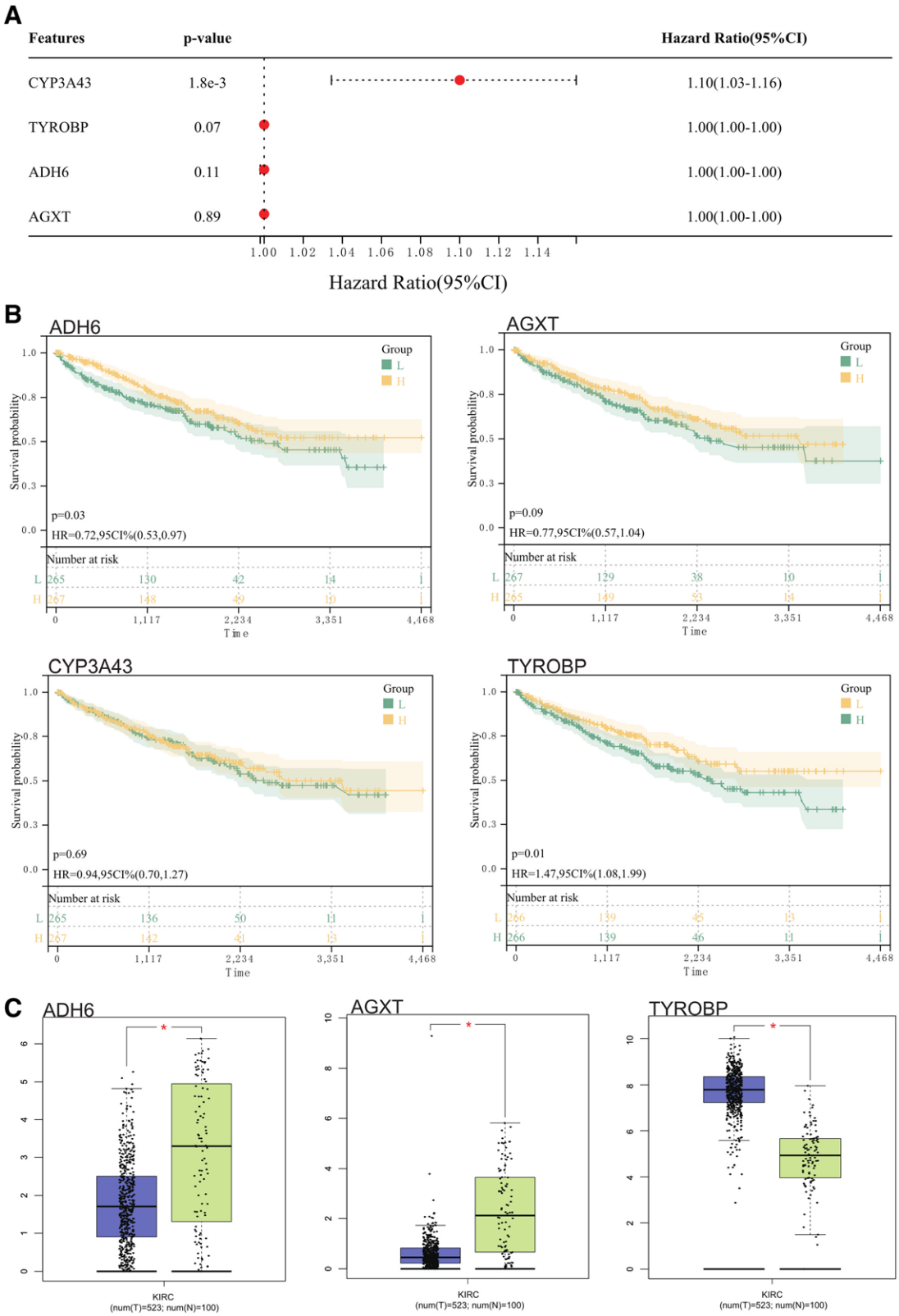

Figure 11. Survival analysis. (A) Forest plot. (B) KM survival curve. (C) Box plot for the core genes.

harmful malignancy, which may continue to grow and spread to other sites if not discovered and treated in a timely manner, resulting in the widespread spread and growth of cancer cells in the body and ultimately endangering the life of patients. Renal cancer is generally highly aggressive and metastatic, causing damage to various systems of the body. Renal cancer may cause pain and discomfort in areas such as the waist, back, abdomen, and bones. The diagnosis and treatment of kidney cancer may cause psychological stress to the patient and family, while it may cause several side effects.[17] Abdominal aortic aneurysms are very harmful, rupture of abdominal aortic aneurysms causes massive internal bleeding, is life-threatening, abdominal

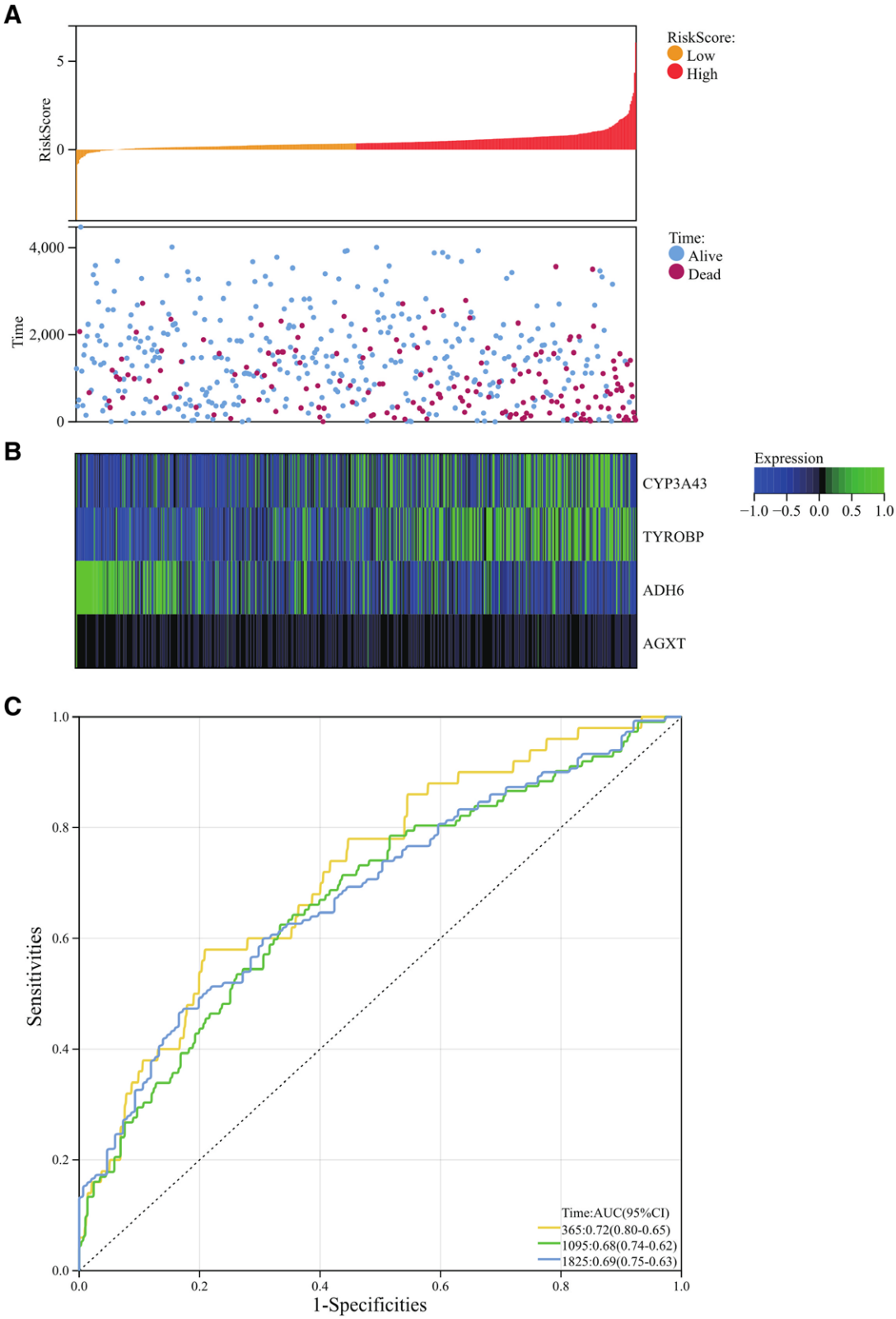

Figure 12. Survival analysis. (A) The prognosis score relationship for renal cell carcinoma. (B) Core gene expression in renal cell carcinoma survival data volume heat maps. (C) ROC curves for the risk score.

aortic aneurysms will form blood clots, block blood vessels, and as abdominal aortic aneurysms enlarge, may compress surrounding tissues and organs.[18] The molecular mechanism of renal cancer is a complex process. The mammalian target of rapamycin (mTOR) signaling pathway plays a role in the regulating cell growth and metabolic processes. MTOR pathway abnormalities commonly observed in renal cancer can lead to cellular hyperproliferation and metabolic abnormalities.[19] Chromosomal deletions common in renal cancer may lead to abnormalities in multiple cancer-related pathways, such as loss

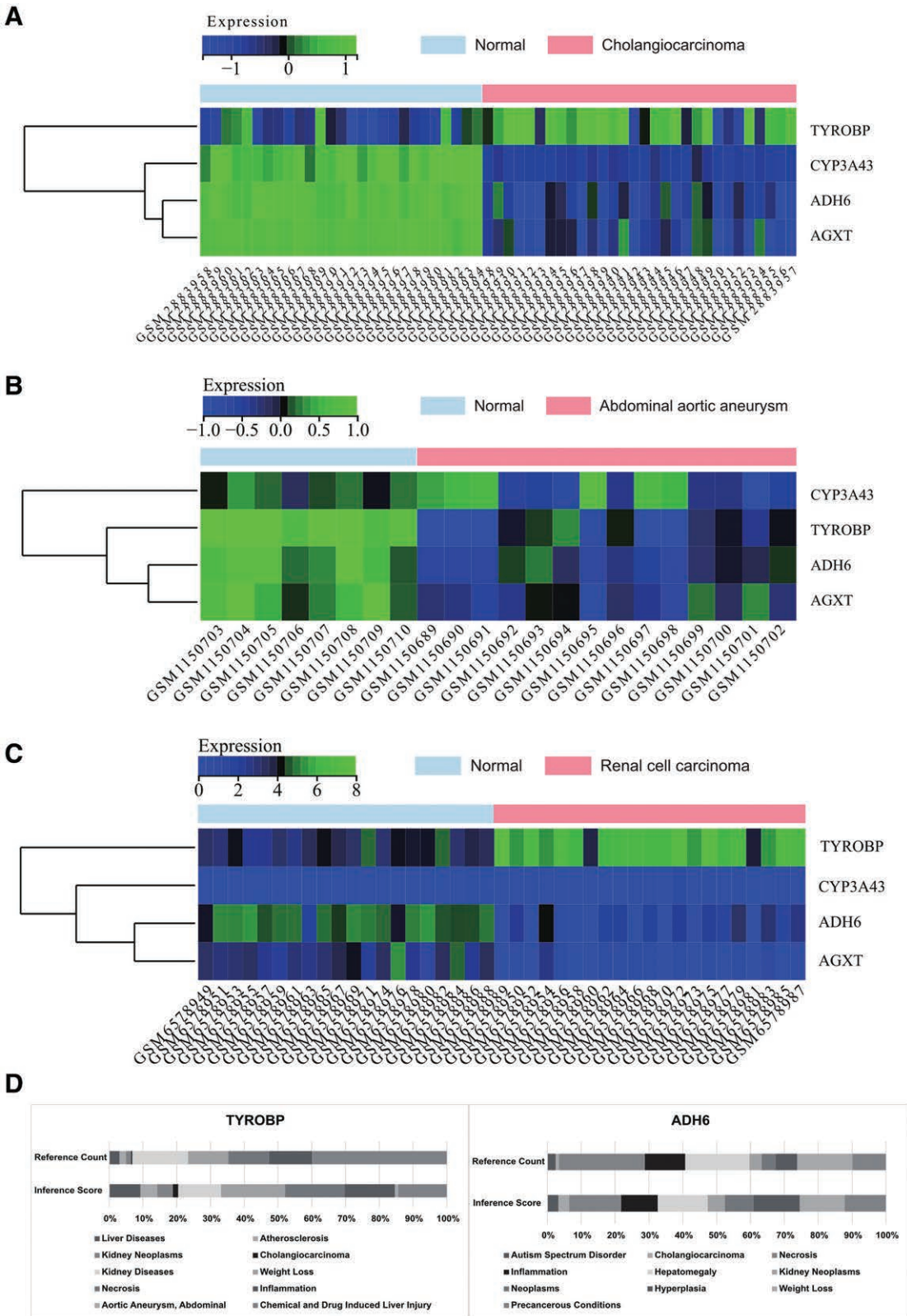

Figure 13. (A) Gene expression heat map of cholangiocarcinoma (B) Gene expression heat map of renal cell carcinoma. (C) Gene expression heat map of abdominal aortic aneurysm. (D) CTD analysis. CTD = comparative toxicogenomics database.

of the tumor suppressor p53, among others.[20,21] There are other genetic mutations in RCC, such as BaP1, setd2, PTEN, TP53 and others. These mutations may lead to abnormalities in biological processes such as tumorigenesis, proliferation, invasion and metastasis.[22] Common epigenetic alterations in renal cancer include DNA methylation and histone modifications, among others. These alterations may lead to abnormal gene expression and thus affect multiple biological processes.[23] The molecular mechanisms underlying abdominal aortic aneurysms include multiple aspects. The inflammatory response triggers a

series of biological events, including the release of cytokines, chemical mediators, which can cause cell apoptosis, degradation of extracellular matrix (ECM) degradation and apoptosis of smooth muscle cell (SMC), leading to structural changes in the aortic wall and ultimately formation of AAA.[24] During the development of AAA, release of a variety of cytokines and mediators caused by inflammatory response can promote expression and activity of MMPs (matrix metalloproteinases) and other proteases in the aortic wall, leading to the degradation of ECM and increased vulnerability of the aortic wall.[25] Under normal conditions, SMCs of the aortic wall are the main components of the aortic wall, and the loss of SMCs and apoptosis of SMCs is one of the main causes of abdominal aortic aneurysm formation. Several factors, such as oxidative stress, inflammatory response and genetic factors, can lead to SMC proliferation and apoptosis, resulting in structural changes of the aortic wall and the formation of abdominal aortic aneurysms.[26] Mutations in tgfbr2, myh11, ACTA2, FLNA, and COL3A1 may lead to abnormal ECM metabolism and abnormal SMC proliferation and apoptosis, which can trigger abdominal aortic aneurysm formation.[27–29] The main results of this study are that TYROBP gene is aberrantly expressed in cholangiocarcinoma, renal cancer and abdominal aortic aneurysm.

The tyrosine protein kinase binding protein (TYROBP) is a transmembrane adaptor molecule consisting of a single transmembrane region and a short intracellular domain. TYROBP mainly plays a role in immune system and regulates the function of immune cells by binding to activating receptors on the cell surface. TYROBP mainly binds to activating receptors of the NKG2 family and regulates activation of natural killer (NK) cells and certain T cell subsets. When TYROBP binds to its activating receptors, it activates several downstream signaling pathways, such as Syk, ZAP-70, and PI3K, which promote cell proliferation, cytokine production, and cytotoxic killing, and TYROBP also binds to other receptors, and plays a role in the regulation of monocytes Biological processes such as macrophages and dendritic cells play a role.[30,31] There are studies suggesting an interaction between TYROBP, Sox6 and renal tumors, with higher inferred scores for TYROBP and Sox6 for renal tumors.[32] The high expression of TYROBP is closely related to the poor prognosis and immune cell infiltration of clear cell renal cell carcinoma.[33] It has also been shown that in vivo experiments revealed that TYROBP is significantly underexpressed in AAA abdominal aortic tissue.[34] Therefore, it is speculated that TYROBP may influence the occurrence and development of cholangiocarcinoma, renal cell carcinoma, and abdominal aortic aneurysm.

Although this paper has carried out rigorous bioinformatics analysis, there are still some shortcomings. Animal experiments with overexpression or knockdown of the gene were not performed in this study to further verify the function.

5. Conclusion

TYROBP is aberrantly expressed in cholangiocarcinoma, renal cancer and abdominal aortic aneurysm and may play a significant role through cellular regulation and other pathways. TYROBP may serve as a molecular target for precision treatment of cholangiocarcinoma, renal cancer and abdominal aortic aneurysm and provide a certain direction basis for mechanistic study

Author contributions

Conceptualization: Lei Chen, Hongru Deng.
Data curation: Wei Jia, Shiyang Hou, Chunbo Kang, Hongru Deng.
Formal analysis: Wei Jia, Shiyang Hou, Chunbo Kang, Hongru Deng.
Methodology: Wei Jia, Shiyang Hou, Chunbo Kang.
Project administration: Lei Chen.
Software: Wei Jia.
Supervision: Lei Chen.
Validation: Lei Chen.
Visualization: Lei Chen.
Writing – original draft: Shiyang Hou, Hongru Deng.
Writing – review & editing: Lei Chen, Shiyang Hou.

References

[1] Brindley PJ, Bachini M, Ilyas SI, et al. Cholangiocarcinoma. Nat Rev Dis Primers. 2021;7:65.
[2] Banales JM, Marin J, Lamarca A, et al. Cholangiocarcinoma 2020: the next horizon in mechanisms and management. Nat Rev Gastroenterol Hepatol. 2020;17:557–88.
[3] Labib PL, Goodchild G, Pereira SP. Molecular pathogenesis of Cholangiocarcinoma. BMC Cancer. 2019;19:185.
[4] Kendall T, Verheij J, Gaudio E, et al. Anatomical, histomorphological and molecular classification of cholangiocarcinoma. Liver Int. 2019;39(Suppl 1):7–18.
[5] Khan SA, Tavolari S, Cholangiocarcinoma BG. Epidemiology and risk factors. Liver Int. 2019;39(Suppl 1):19–31.
[6] Umer M, Mohib Y, Atif M, et al. Skeletal metastasis in renal cell carcinoma: a review. Ann Med Surg (Lond). 2018;27:9–16.
[7] Al Aradi A, Al Rashed AA, Mubarak M, et al. Renal Carcinoma patterns and prevalence in Bahrain: a descriptive study. Cureus. 2022;14:e31443.
[8] Thouvenin J, Barthélémy P, Ladoire S. [Non-clear cell renal cell carcinoma: clinico-biological characteristics and therapeutic management except surgery]. Bull Cancer. 2020;107:S56–65.
[9] Lopez-Beltran A, Cheng L, Vidal A, et al. Pathology of renal cell carcinoma: an update. Anal Quant Cytopathol Histpathol. 2013;35:61–76.
[10] Fernandes DS, Lopes JM. Pathology, therapy and prognosis of papillary renal carcinoma. Future Oncol. 2015;11:121–32.
[11] Keisler B, Carter C. Abdominal aortic aneurysm. Am Fam Physician. 2015;91:538–43.
[12] Sprynger M, Willems M, Van Damme H, et al. Screening program of abdominal aortic aneurysm. Angiology. 2019;70:407–13.
[13] Sonesson B, Dias N, Resch T. Is there an age limit for abdominal aortic aneurysm repair. J Cardiovasc Surg (Torino). 2018;59:190–4.
[14] Haque K, Bhargava P. Abdominal aortic aneurysm. Am Fam Physician. 2022;106:165–72.
[15] Torres-Fonseca M, Galan M, Martinez-Lopez D, et al.; En representación del Grupo de trabajo de Biología Vascular de la Sociedad Española de Arteriosclerosis. Pathophisiology of abdominal aortic aneurysm: biomarkers and novel therapeutic targets. Clin Investig Arterioscler. 2019;31:166–77.
[16] Khan AS, Dageforde LA. Cholangiocarcinoma. Surg Clin North Am. 2019;99:315–35.
[17] Gambuti E, Alfano F, Fabbian F, et al. Subcutaneous emphysema as a life-threatening complication of metastatic renal cancer: a case report. Curr Health Sci J. 2021;47:466–8.
[18] Wilkinson DA, Daou BJ, Nadel JL, et al. Abdominal aortic aneurysm is associated with subarachnoid hemorrhage. J Neurointerv Surg. 2021;13:716–21.
[19] Cao C, Wang Y, Wu X, et al. The roles and mechanisms of circular RNAs related to mTOR in cancers. J Clin Lab Anal. 2022;36:e24783.
[20] Zhang H, Ye Q, Du Z, et al. MiR-148b-3p inhibits renal carcinoma cell growth and pro-angiogenic phenotype of endothelial cell potentially by modulating FGF2. Biomed Pharmacother. 2018;107:359–67.
[21] Warburton HE, Brady M, Vlatković N, et al. p53 regulation and function in renal cell carcinoma. Cancer Res. 2005;65:6498–503.
[22] Shao YF, DeBenedictis M, Yeaney G, et al. Germ line BAP1 mutation in patients with uveal melanoma and renal cell carcinoma. Ocul Oncol Pathol. 2021;7:340–5.
[23] Minardi D, Lucarini G, Filosa A, et al. Do DNA-methylation and histone acetylation play a role in clear cell renal carcinoma? Analysis of radical nephrectomy specimens in a long-term follow-up. Int J Immunopathol Pharmacol. 2011;24:149–58.
[24] Hellmann DB, Grand DJ, Freischlag JA. Inflammatory abdominal aortic aneurysm. JAMA. 2007;297:395–400.
[25] Pearce WH, Shively VP. Abdominal aortic aneurysm as a complex multifactorial disease: interactions of polymorphisms of inflammatory genes, features of autoimmunity, and current status of MMPs. Ann NY Acad Sci. 2006;1085:117–32.

[26] Jiang B, Wang M, Li X, et al. Hexarelin attenuates abdominal aortic aneurysm formation by inhibiting SMC phenotype switch and inflammasome activation. Microvasc Res. 2022;140:104280.
[27] Biros E, Norman PE, Jones GT, et al. Meta-analysis of the association between single nucleotide polymorphisms in TGF-β receptor genes and abdominal aortic aneurysm. Atherosclerosis. 2011;219:218–23.
[28] Ware SM, Shikany A, Landis BJ, et al. Twins with progressive thoracic aortic aneurysm, recurrent dissection and ACTA2 mutation. Pediatrics. 2014;134:e1218–23.
[29] Zhang W, Han Q, Zhou M, et al. Identification of a missense mutation of COL3A1 in a Chinese family with atypical Ehlers-Danlos syndrome using targeted next-generation sequencing. Mol Med Rep. 2017;15:936–40.
[30] Wang L, Lin Y, Yuan Y, et al. Identification of TYROBP and FCER1G as key genes with prognostic value in clear cell renal cell carcinoma by bioinformatics analysis. Biochem Genet. 2021;59:1278–94.
[31] Tomasello E, Vivier E. KARAP/DAP12/TYROBP: three names and a multiplicity of biological functions. Eur J Immunol. 2005;35:1670–7.
[32] Lv XQ, Zhang KB, Guo X, et al. Higher TYROBP and lower SOX6 as predictive biomarkers for poor prognosis of clear cell renal cell carcinoma: a pilot study. Medicine (Baltimore). 2022;101:e30658.
[33] Wu P, Xiang T, Wang J, et al. TYROBP is a potential prognostic biomarker of clear cell renal cell carcinoma. FEBS Open Bio. 2020;10:2588–604.
[34] Li Y, Li R, Guo S, et al. Bioinformatics-based identification of lipid- and immune-related biomarkers in abdominal aortic aneurysms. Heliyon. 2023;9:e13622.